Fe_3O_4 polyhedral nanoparticles with a high magnetization synthesized in mixed solvent ethylene glycol–water system

Shao-Wen Cao, Ying-Jie Zhu* and Jiang Chang

Received (in Gainesville, FL, USA) 17th December 2007, Accepted 7th April 2008
First published as an Advance Article on the web 7th May 2008
DOI: 10.1039/b719436f

We report a solvothermal approach for the synthesis of high-magnetization Fe_3O_4 polyhedral nanoparticles in the ethylene glycol (EG)–H_2O system. In this approach, ferric chloride ($FeCl_3 \cdot 6H_2O$) is used as the iron source, and EG acts as both the solvent and reductant in the presence of sodium hydroxide (NaOH) and dodecylamine (DDA). The presence of deionized water plays an important role in the control over the size of Fe_3O_4 particles. The Fe_3O_4 particles prepared are well dispersed with single-crystal-like features, showing superparamagnetism with a high saturation magnetization close to that of bulk Fe_3O_4 (92 emu g^{-1}). The stability of the Fe_3O_4 nanoparticles in deionized water is also investigated.

1 Introduction

During the past decades, nanostructured materials have attracted considerable attention due to their fundamental significance for physical properties and potential applications.[1–4] Much effort has been made to study their novel physical properties (such as electronic, magnetic and optical traits) as well as the quantum confinement effect and space confined transport phenomena, which differ from those of their bulk counterparts.[5–7] It is well known that the properties of nanomaterials are affected not only by their chemical composition, but also by their structure, shape and size.[8] Magnetic nanocrystals have been of keen interest in the applications such as magnetic recording media, magnetic resonance imaging (MRI), and targeted drug delivery.[9–11] Moreover, the synthesis of magnetic nanomaterials with a controlled size and morphology has been of scientific and technological interest. Indeed, the reduction in the particle size leads to new and novel properties, particularly magnetic properties (superparamagnetism).[12,13]

The intriguing potential applications of magnetic nanostructures have stimulated the rapid development of the synthetic techniques. To date, a variety of synthetic methods for magnetic nanoparticles have been developed, such as chemical co-precipitation,[14] inverse microemulsion,[15] ultrasound irradiation,[16] laser pyrolysis,[17] thermal decomposition,[18–20] microwave-assisted method[21,22] and solvothermal method.[23] Various magnetic nanostructures with different morphologies have been synthesized, such as monodisperse nanoparticles,[24–27] microspheres,[28] nanorods,[29–31] nanowires,[32,33] nanosheets[21] and nanotubes.[34,35] Although magnetic nanostructures with different morphologies have been prepared, controlled synthesis of magnetic (especially high magnetization) nanoscale crystals with various morphologies always turns out to be a great challenge to scientists. The size, shape, surface defect, and phase purity are only a few of the parameters influencing the magnetic properties, which makes the investigation of the magnetism very complicated. One of the great challenges remains the manufacturing of magnetic nanostructures with well-defined shape, controlled composition, ideal chemical stability, tunable interparticle separations, high magnetization and a functionalizable surface. Thus, the synthesis of magnetic nanostructures with well-controlled characteristics is a very important task.[36]

Herein we report a solvothermal approach for the controlled synthesis of high-magnetization Fe_3O_4 nanoparticles in an ethylene glycol (EG)–H_2O system. To the best of our knowledge, this is the first report on a simple one-step controlled synthesis of high-magnetization Fe_3O_4 polyhedral nanoparticles in the ethylene glycol (EG)–H_2O system. In this approach, ferric chloride ($FeCl_3 \cdot 6H_2O$) is used as the iron source, and EG acts as both a solvent and reductant in the presence of sodium hydroxide (NaOH) and dodecylamine (DDA). The Fe_3O_4 particles prepared are well dispersed and with single-crystal-like features, showing superparamagnetism with a high saturation magnetization close to that of bulk Fe_3O_4 (92 emu g^{-1}). The Fe_3O_4 polyhedral nanoparticles have a good stability in aqueous solution.

2 Experimental

All chemicals used in our experiments were purchased and used as received without further purification. Ferric chloride ($FeCl_3 \cdot 6H_2O$), ethylene glycol (EG) and dodecylamine (DDA) were purchased from Sinopharm Chemical Reagent Co., Ltd. Sodium hydroxide (NaOH) was purchased from Shanghai Ling-Feng Chemical Reagent Co., Ltd.

In the typical synthetic procedure of the Fe_3O_4 samples, solution A was prepared by dissolving 0.541 g of $FeCl_3 \cdot 6H_2O$ and 0.371 g of DDA in 20 mL of EG under magnetic stirring at a rate of *ca.* 750 rpm at 50 °C, and solution B was prepared by dissolving 0.160 g of NaOH in 10 mL of EG under magnetic stirring at a rate of *ca.* 750 rpm at 50 °C. Then the two solutions were mixed together and different dosages of

State Key Laboratory of High Performance Ceramics and Superfine Microstructure, Shanghai Institute of Ceramics, Chinese Academy of Sciences, Shanghai, 200050, P. R. China and Graduate School of Chinese Academy of Sciences, Beijing, 100049, P. R. China. E-mail: y.j.zhu@mail.sic.ac.cn; Fax: +86 21-52413122; Tel: +86 21-52412616

Table 1 Experimental parameters for the synthesis of typical samples (hydrothermal temperature was 220 °C for all samples)

Sample	Solvent	*t*/h	Morphology	Size/nm
1	EG (30 ml) + H_2O (1 ml)	12	Polyhedra	234.5 (av.)
2	EG (30 ml) + H_2O (1 ml)	18	Polyhedra	99.3 (av.)
3	EG (30 ml)	12	Hollow spheres	*ca.* 250
4	EG (30 ml)	18	Hollow spheres	*ca.* 250
5	EG (30 ml) + H_2O (2 ml)	12	Polyhedra	46.8 (av.)
6	EG (30 ml) + H_2O (3 ml)	12	Irregular	15–30

deionized water were added to the mixture under magnetic stirring at a rate of *ca.* 750 rpm at room temperature, leading to the formation of a yellow suspension. The resultant solution was loaded into a 50 mL-Teflon lined stainless steel autoclave, sealed, and heated at 220 °C for a period of time. The black solid product was obtained by centrifugation, washed with water and ethanol three times, and dried. The detailed experimental parameters for the synthesis of typical samples are listed in Table 1.

To examine the stability of the Fe_3O_4 samples, the as-prepared samples (20 mg) were dispersed in deionized water (100 mL) by sonication and their stability monitored with time.

X-Ray powder diffraction (XRD) patterns were recorded using a Rigaku D/max 2550 V X-ray diffractometer with high-intensity Cu-Kα radiation (λ = 1.54178 Å) and a graphite monochromator. The transmission electron microscopy (TEM) micrographs and selected-area electron diffraction (SAED) patterns were taken with a Hitachi H-800 transmission electron microscope with an accelerating voltage of 200 kV. Scanning electron microscopy (SEM) images was recorded on a JSM-6700F field emission scanning electron microscope. A physical property measurement system (PPMS) (USA) was used to evaluate the magnetic properties at room temperature. Thermogravimetric analysis (TG) curves were measured with a heating rate of 10 °C min^{-1} in a flowing N_2 atmosphere with a STA 409/PC simultaneous thermal analyzer (Netzsch, Germany).

3 Results and discussion

Ethylene glycol is a reducing agent with a relatively high boiling point, and has been widely used in the polyol process to prepare fine metal or metal oxide materials.[37–40] The solvothermal process is one of the successful ways of growing crystals of many different materials. This technique has also been used to grow dislocation-free single-crystalline particles, and crystals formed in this process have a better crystallinity than those from other processes. Thus, we synthesized Fe_3O_4 nanostructures combining the advantages of ethylene glycol and the solvothermal process.

The black products were characterized by X-ray powder diffraction (XRD). As shown in Fig. 1, the XRD patterns can be indexed to Fe_3O_4 (JCPDS No. 19-0629), indicating that Fe_3O_4 can be obtained by such a simple solvothermal reduction method.

Samples 1 and 2 were synthesized for 12 and 18 h in the presence of 1 mL deionized water. Fig. 2(a) and (b) shows the

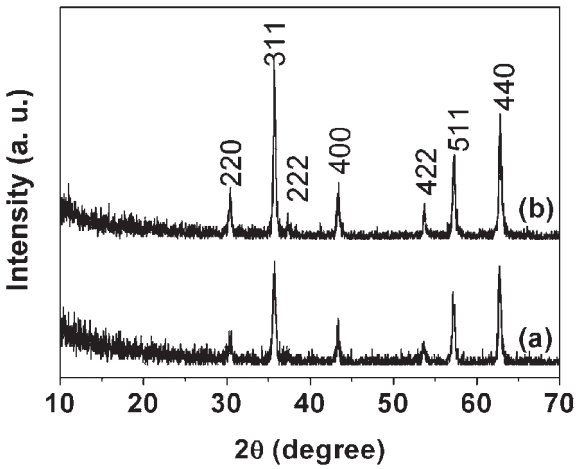

Fig. 1 XRD patterns of Fe_3O_4 samples: (a) sample 1; (b) sample 5.

typical SEM micrographs of sample 1, from which one can see the polyhedral shape. In some cases, there are also nanoparticles with holes in them (middle of Fig. 2(b)) and bowl-like structures (middle left of Fig. 2(b)) which suggest that there are some hollow nanoparticles. Fig. 2(c) and (d) show TEM micrographs of sample 1, and Fig. 2(g) shows the histogram of the particle size distribution of sample 1. The diameters of the polyhedral particles ranged from 150 to 280 nm, and the average diameter was 234.5 nm. The SAED pattern in the inset of Fig. 2(c) reveals the single-crystal-like feature of the polyhedral particles. The inset of Fig. 2(d) suggests that each polyhedral particle is comprised of many small nanoparticles. According to the Scherrer equation, the average crystallite size calculated based on the XRD pattern is approximately 21.0 nm. The above information also indicated an oriented aggregation of Fe_3O_4 nanoparticles.[41] The main driving force for oriented aggregation of nanoparticles can be generally attributed to the tendency for reducing the high surface energy through both the attachment among the primary nanoparticles and the rotation of the primary nanoparticles caused by various interactions such as Brownian motion, and the short-range interactions between adjacent surfaces, *i.e.*, oriented aggregation.[42–44] There are also some polyhedral particles that exhibit the "ring" appearance of shell nanoparticles (bottom of Fig. 2(d)), which confirm that there are also some hollow nanoparticles. Fig. 2(e) and (f) show TEM micrographs of sample 2. Surprisingly, the size of the Fe_3O_4 polyhedral particles significantly decreased, but the morphology was similar to that of sample 1. Fig. 2(h) shows the histogram of the particle size distribution of sample 2. The diameters of the polyhedral particles ranged from 70 to 120 nm, and the average diameter was 99.3 nm.

In comparison, the samples synthesized without adding deionized water were also investigated. Following the procedure reported by Yu *et al.*,[45] samples 3 and 4 were synthesized for 12 and 18 h, respectively, without adding deionized water. Fig. 3(a) and (b) show the typical SEM micrographs of sample 3, from which one can see that the Fe_3O_4 product consisted of hollow microspheres assembled by small nanoparticles. The average size of the hollow spheres was around 250 nm.

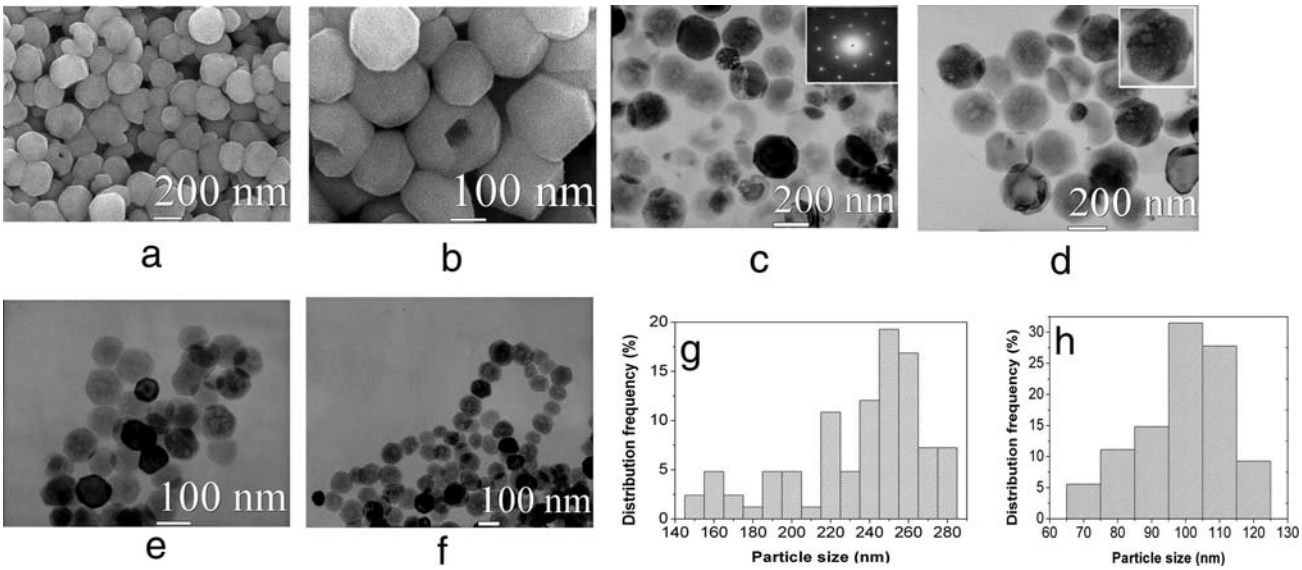

Fig. 2 (a) and (b) SEM micrographs of sample 1; (c) and (d) TEM micrographs of sample 1, the inset of (c) is the corresponding SAED pattern; (e) and (f) TEM micrographs of sample 2; (g) the histogram of particle size distribution of sample 1; (h) the histogram of particle size distribution of sample 2.

Fig. 3(c) and (d) show TEM micrographs of sample 3, which confirm the hollow structures. The SAED pattern in the inset of Fig. 3(c) reveals the single-crystal-like feature of these hollow microspheres, indicating an oriented aggregation of Fe_3O_4 nanoparticles. Fig. 3(e) and (f) show SEM and TEM micrographs of sample 4. One can see that the shape and size of the Fe_3O_4 hollow spheres are similar to those of sample 3. However, the size of the Fe_3O_4 polyhedral particles significantly decreased in the presence of deionized water, as discussed above. This result indicates the significant influence of the addition of deionized water.

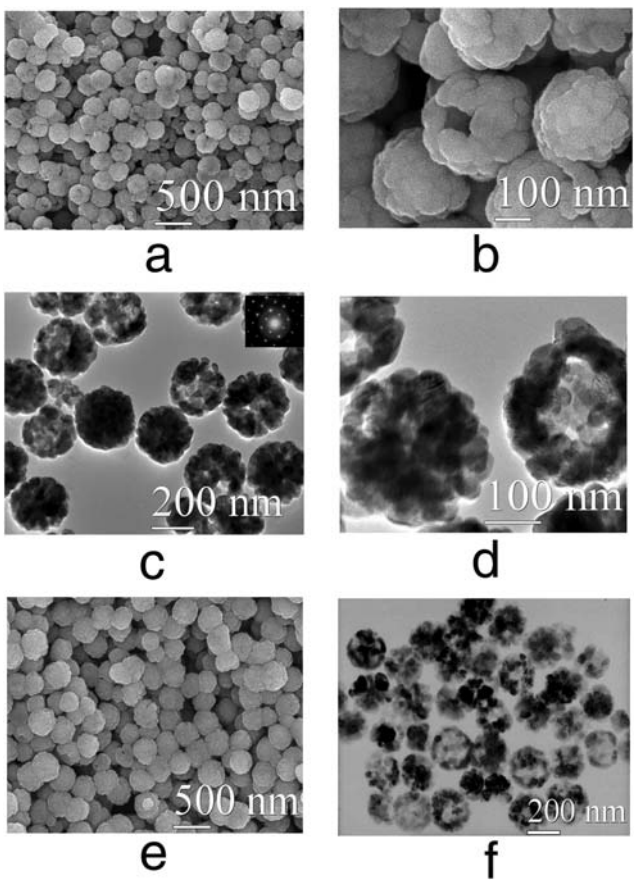

Fig. 3 (a) and (b) SEM micrographs of sample 3; (c) and (d) TEM micrographs of sample 3, the inset of (c) is the corresponding SAED pattern; (e) SEM micrograph of sample 4; and (f) TEM micrograph of sample 4.

In the formation process of Fe_3O_4 polyhedral particles, $FeCl_3{\cdot}6H_2O$ is used as the iron source, and EG acts as both a solvent and reductant. Furthermore, NaOH and water play an important role in the formation process of Fe_3O_4. It has been reported that Fe^{3+} can not be reduced by ethylene glycol alone.[28] Yu *et al.*[45] have observed that in the absence of deionized water in the reaction system, the morphology of Fe_3O_4 nanoparticles changed in the following sequence as the concentration of DDA increased: rhombic particles, solid spheres, hollow microspheres, large-size solid spheres and irregular particles. In our EG–H_2O reaction system, DDA also serves to form the surfactant micelles, thus controlling the morphology of Fe_3O_4 particles. The most important factor is the presence of deionized water in the reaction system. In the non-aqueous system, the addition of water provides a simple method to prepare oxide nanoparticles with controlled size and narrow size distribution.[42] Because the coordination of water molecules to metal ions is stronger than that of EG molecules, the coordinated EG molecules will be substituted by water molecules when water is added into the reaction solution. By adjusting the dosage of deionized water, the particle size and size distribution of Fe_3O_4 nanoparticles can be controlled.

In order to get more information about the effect of deionized water, we synthesized samples 5 and 6 for 12 h in the presence of 2 and 3 mL deionized water in the reaction system, respectively. Fig. 4(a)–(d) show typical SEM and TEM

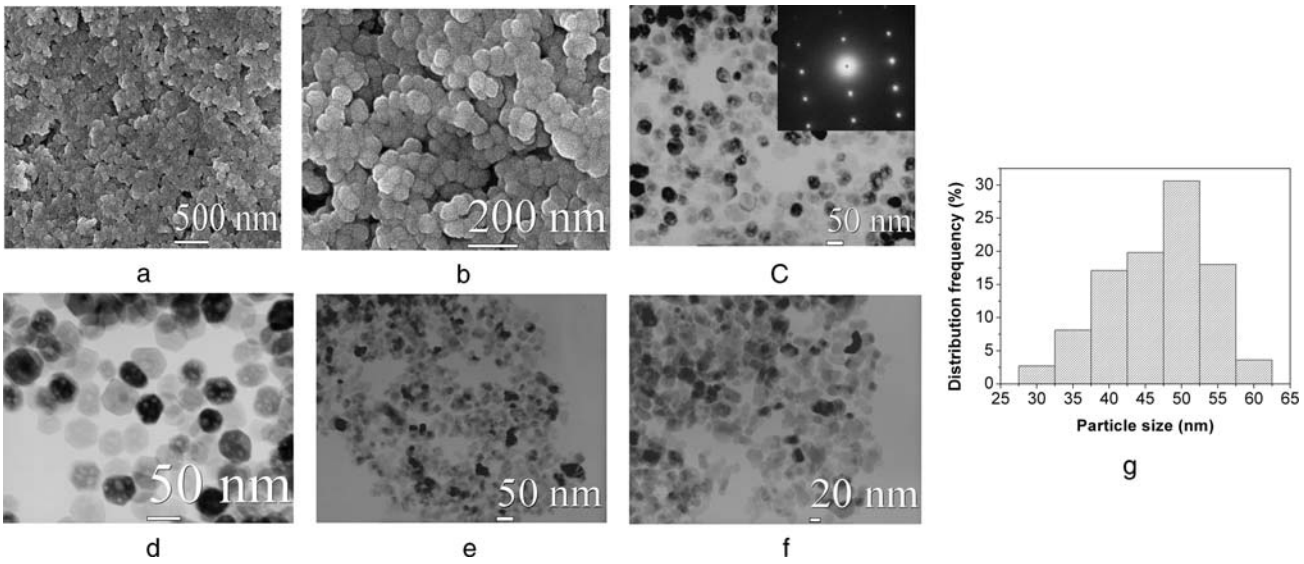

Fig. 4 (a) and (b) SEM micrographs of sample 5; (c) and (d) TEM micrographs of sample 5, the inset of (c) is the corresponding SAED pattern; (e) and (f) TEM micrographs of sample 6; (g) the histogram of particle size distribution of sample 5.

micrographs of sample 5. The sizes of the Fe_3O_4 polyhedral nanoparticles decreased with little change in the morphology. Fig. 4(g) shows the histogram of the particle size distribution of sample 5. The diameters of the polyhedral particles ranged from 30 to 60 nm, and the average diameter was 46.8 nm. The SAED pattern in the inset of Fig. 4(c) reveals the single-crystal-like feature of the polyhedral nanoparticles. According to the Scherrer equation, the average crystallite size calculated based on the XRD pattern is approximately 14.3 nm. Fig. 4(e) and (f) show the TEM micrographs of sample 6, from which one can see that the sizes of Fe_3O_4 nanoparticles were in the range of 15–30 nm, and the morphology became irregular. These results indicate the significant effect of deionized water on the formation of Fe_3O_4 nanostructures.

The magnetic properties of Fe_3O_4 polyhedral nanoparticles (samples 1 and 5) were also investigated. The room-temperature magnetization curves are shown in Fig. 5. Both samples exhibited a superparamagnetic characteristic. The result that these large polyhedral particles are superparamagnetic is owing to the fact that they are comprised of many small nanoparticles that show oriented aggregation into a superstructure. The polyhedral nanoparticles of sample 5 have a high saturation magnetization M_s of 83.8 emu g^{-1}. The Fe_3O_4 polyhedral particles of sample 1 have an even higher saturation magnetization M_s of 90.3 emu g^{-1}.

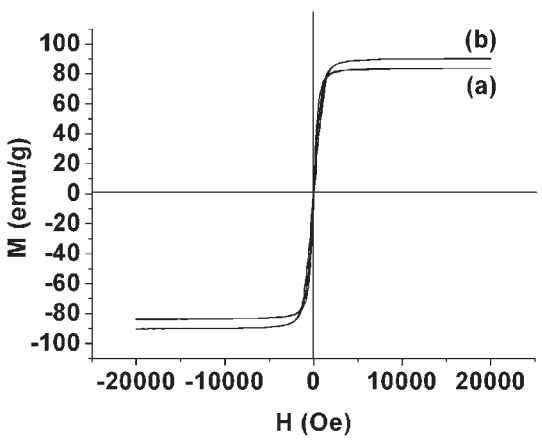

Fig. 5 The magnetization curves measured at room temperature for the Fe_3O_4 samples: (a) sample 5; (b) sample 1.

The saturation magnetization M_s = 90.3 emu g^{-1} of sample 1 is very high at room temperature, slightly smaller than that of bulk Fe_3O_4 (92 emu g^{-1}). Only a few papers have reported values above 90 emu g^{-1}.[31,46] It can be observed that the saturation magnetization decreased as the size decreased. This agrees with the known fact that the magnetization of small particles decreases as the particle size decreases.[47,48] Sample 5 consisted of nanoparticles smaller than those of sample 1.

To investigate the stability of the Fe_3O_4 samples, the as-prepared samples (1, 5) (20 mg) were dispersed in deionized water (100 mL) by sonication and the time in which Fe_3O_4 polyhedral particles were retained in the suspension (stability time) was measured. The stability time of samples 1 and 5 was 4 and 7 h, respectively, indicating that the prepared Fe_3O_4 polyhedral particles can be well dispersed in aqueous solution and have a good stability. Therefore, with the appropriate surface modifications, these Fe_3O_4 polyhedral particles may be suitable for applications in clinical diagnosis and in the targeted delivery of drugs, proteins, viruses or bacteria. The TG curve of sample 5 in a flowing N_2 atmosphere is shown in Fig. 6, which shows that there are several mass loss stages and the total mass loss between 190 and 700 °C was around 6%. Here we propose that the total mass loss corresponds to the removal of EG and oxidized products of EG which were adsorbed on the nanoparticle surface and played an important role as stabilizer for the Fe_3O_4 nanoparticles. The stability of the Fe_3O_4 powders (samples 1 and 5) in ethanol was also investigated. However, these Fe_3O_4 polyhedral particles exhibited poor stability in ethanol and both samples precipitated completely within 1 h.

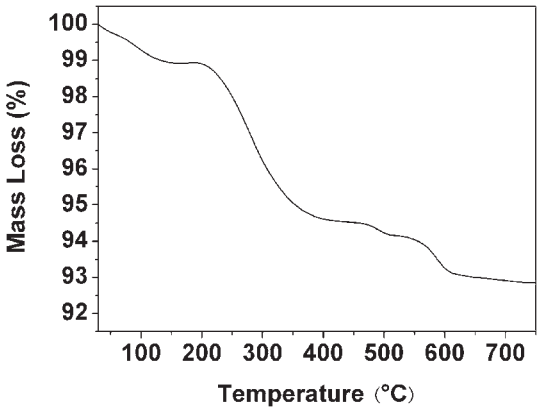

Fig. 6 The TG curve of sample 5 in a flowing N_2 atmosphere.

Conclusion

We have demonstrated a simple solvothermal reduction method in the ethylene glycol (EG)–H_2O system for the preparation of high-magnetization Fe_3O_4 polyhedral nanoparticles. In this method, the water plays an important role in the formation of polyhedral Fe_3O_4 particles with different sizes. The addition of water with different dosage into the reaction system causes the formation of Fe_3O_4 polyhedral nanoparticles with different size. The Fe_3O_4 polyhedral particles prepared can be well dispersed in aqueous solution and show a good stability. The magnetic property measurements show superparamagnetism with a very high saturation magnetization close to the value of bulk Fe_3O_4 (92 emu g^{-1}). Moreover, the saturation magnetization of these materials change regularly with the size. The synthetic strategy developed in this study may also be extended to the preparation of other magnetic nanomaterials.

Acknowledgements

Financial support from the National Natural Science Foundation of China (50772124, 50472014), the Program of Shanghai Subject Chief Scientist (07XD14031), the Key Project for Innovative Research (SCX0606) and Director Fund of Biomaterials Research Center from Shanghai Institute of Ceramics is gratefully acknowledged.

References

1 J. T. Hu, T. W. Odom and C. M. Lieber, *Acc. Chem. Res.*, 1999, **32**, 435.
2 A. P. Alivisatos, *Science*, 1996, **271**, 933.
3 T. S. Ahmadi, Z. L. Wang, T. C. Green, A. Henglein and M. A. El-Sayed, *Science*, 1996, **272**, 1924.
4 X. Duan, Y. Huang, Y. Cui, J. Wang and C. M. Lieber, *Nature*, 2001, **409**, 66.
5 Z. B. Zhang, X. Z. Sun, M. S. Dresselhaus and J. Y. Ying, *Phys. Rev. B: Condens. Matter Mater. Phys.*, 2000, **61**, 4850.
6 Z. L. Wang, *Adv. Mater.*, 2000, **12**, 1295.
7 Y. Cui, Q. Q. Wei, H. K. Park and C. M. Lieber, *Science*, 2001, **293**, 1289.
8 A. P. Alivisatos, *J. Phys. Chem.*, 1996, **100**, 13226.
9 F. Caruso, M. Spasova, A. Susha, M. Giersig and R. A. Caruso, *Chem. Mater.*, 2001, **13**, 109.
10 T. Hyeon, S. S. Lee, J. Park, Y. Chung and H. B. Na, *J. Am. Chem. Soc.*, 2001, **123**, 12798.
11 S. H. Yu and M. Yoshimura, *Adv. Funct. Mater.*, 2002, **12**, 9.
12 K. Raj and R. J. Moskowitz, *J. Magn. Magn. Mater.*, 1990, **85**, 233.
13 D. L. Leslie-Pelecky and R. D. Rieke, *Chem. Mater.*, 1996, **8** 1770.
14 L. A. Harris, J. D. Goff, A. Y. Carmichael, J. S. Riffle, J. J. Harburn, T. G. S. Pierre and M. Saunders, *Chem. Mater.*, 2003, **15**, 1367.
15 S. Mann, H. C. Sparks and R. G. Board, *Adv. Microb. Physiol.*, 1990, **31**, 125.
16 R. V. Kumar, Y. Koltypin, X. N. Xu, Y. Yeshurun, A. Gedanken and I. Felner, *J. Appl. Phys.*, 2001, **89**, 6324.
17 S. V. Verdaguer, O. B. Miguel and M. P. Morales, *Scr. Mater.*, 2002, **47**, 589.
18 S. H. Sun and H. Zeng, *J. Am. Chem. Soc.*, 2002, **124**, 8204.
19 J. Park, K. An, Y. Hwang, J. G. Park, H. J. Noh, J. Y. Kim, J. H. Park, N. M. Hwang and T. Hyeon, *Nat. Mater.*, 2004, **3**, 891.
20 J. Park, E. Lee, N. M. Hwang, M. Kang, S. C. Kim, Y. Hwang, J. G. Park, H. J. Noh, J. Y. Kim, J. H. Park and T. Hyeon, *Angew. Chem., Int. Ed.*, 2005, **44**, 2872.
21 W. W. Wang and Y. J. Zhu, *Curr. Nanosci.*, 2007, **3**, 171.
22 W. W. Wang, Y. J. Zhu and M. L. Ruan, *J. Nanopart. Res.*, 2007, **9**, 419.
23 S. B. Cho, J. S. Noh, S. J. Park, D. Y. Lim and S. H. Choi, *J. Mater. Sci.*, 2007, **42**, 4877.
24 X. Liang, X. Wang, J. Zhuang, Y. T. Chen, D. S. Wang and Y. D. Li, *Adv. Funct. Mater.*, 2006, **16**, 1805.
25 T. J. Daou, G. Pourroy, S. Bégin-Colin, J. M. Grenèche, C. Ulhaq-Bouillet, P. Legaré, P. Bernhardt, C. Leuvrey and G. Rogez, *Chem. Mater.*, 2006, **18**, 4399.
26 S. F. Si, C. H. Li, X. Wang, D. P. Yu, Q. Peng and Y. D. Li, *Cryst. Growth Des.*, 2005, **5**, 391.
27 W. W. Yu, J. C. Falkner, C. T. Yavuz and V. L. Colvin, *Chem. Commun.*, 2004, 2306.
28 H. Deng, X. L. Li, Q. Peng, X. Wang, J. P. Chen and Y. D. Li, *Angew. Chem., Int. Ed.*, 2005, **44**, 2782.
29 L. Feng, L. Jiang, Z. H. Mai and D. B. Zhu, *J. Colloid Interface Sci.*, 2004, **278**, 372.
30 J. R. Morber, Y. Ding, M. S. Haluska, Y. Li, P. Liu, Z. L. Wang and R. L. Snyder, *J. Phys. Chem. B*, 2006, **110**, 21672.
31 J. Wang, Z. M. Peng, Y. J. Huang and Q. W. Chen, *J. Cryst. Growth*, 2004, **263**, 616.
32 J. Wang, Q. W. Chen, C. Zeng and B. Y. Hou, *Adv. Mater.*, 2004, **16**, 137.
33 Z. B. Huang, Y. Q. Zhang and F. Q. Tang, *Chem. Commun.*, 2005, 342.
34 Y. C. Sui, R. Skomski, K. D. Sorge and D. J. Sellmyer, *Appl. Phys. Lett.*, 2004, **84**, 1525.
35 Y. C. Sui, R. Skomski, K. D. Sorge and D. J. Sellmyer, *Appl. Phys. Lett.*, 2004, **95**, 7151.
36 A. H. Lu, E. L. Salabas and F. Schüth, *Angew. Chem., Int. Ed.*, 2007, **46**, 1222.
37 B. Wiley, T. Herricks, Y. G. Sun and Y. N. Xia, *Nano Lett.*, 2004, **4**, 1733.
38 X. C. Jiang, Y. L. Wang, T. Herricks and Y. N. Xia, *J. Mater. Chem.*, 2004, **14**, 695.
39 D. Larcher and R. Partrice, *J. Solid State Chem.*, 2000, **154** 405.
40 X. M. Sun and Y. D. Li, *Angew. Chem., Int. Ed.*, 2004, **43**, 597.
41 G. Oskam, A. Nellore, R. L. Penn and P. C. Searson, *J. Phys. Chem. B*, 2003, **107**, 1734.
42 T. He, D. R. Chen and X. L. Jiao, *Chem. Mater.*, 2004, **16**, 737.
43 J. F. Banfield, S. A. Welch, H. Zhang, T. T. Ebert and R. L. Penn, *Science*, 2000, **289**, 751.
44 A. P. Alivisatos, *Science*, 2000, **289**, 736.
45 D. B. Yu, X. Q. Sun, J. W. Zou, Z. R. Wang, F. Wang and K. Tang, *J. Phys. Chem. B*, 2006, **110**, 21667.
46 S. H. Xuan, L. Y. Hao, W. Q. Jiang, L. Song, Y. Hu, Z. Y. Chen, L. F. Fei and T. W. Li, *Cryst. Growth Des.*, 2007, **7**, 430.
47 L. Liz, M. A. L. Quintela, J. Mira and J. Rivas, *J. Mater. Sci.*, 1994, **29**, 3797.
48 S. Santra, R. Tapec, N. Theodoropoulou, J. Dobson, A. Hebard and W. H. Tan, *Langmuir*, 2001, **17**, 2900.

